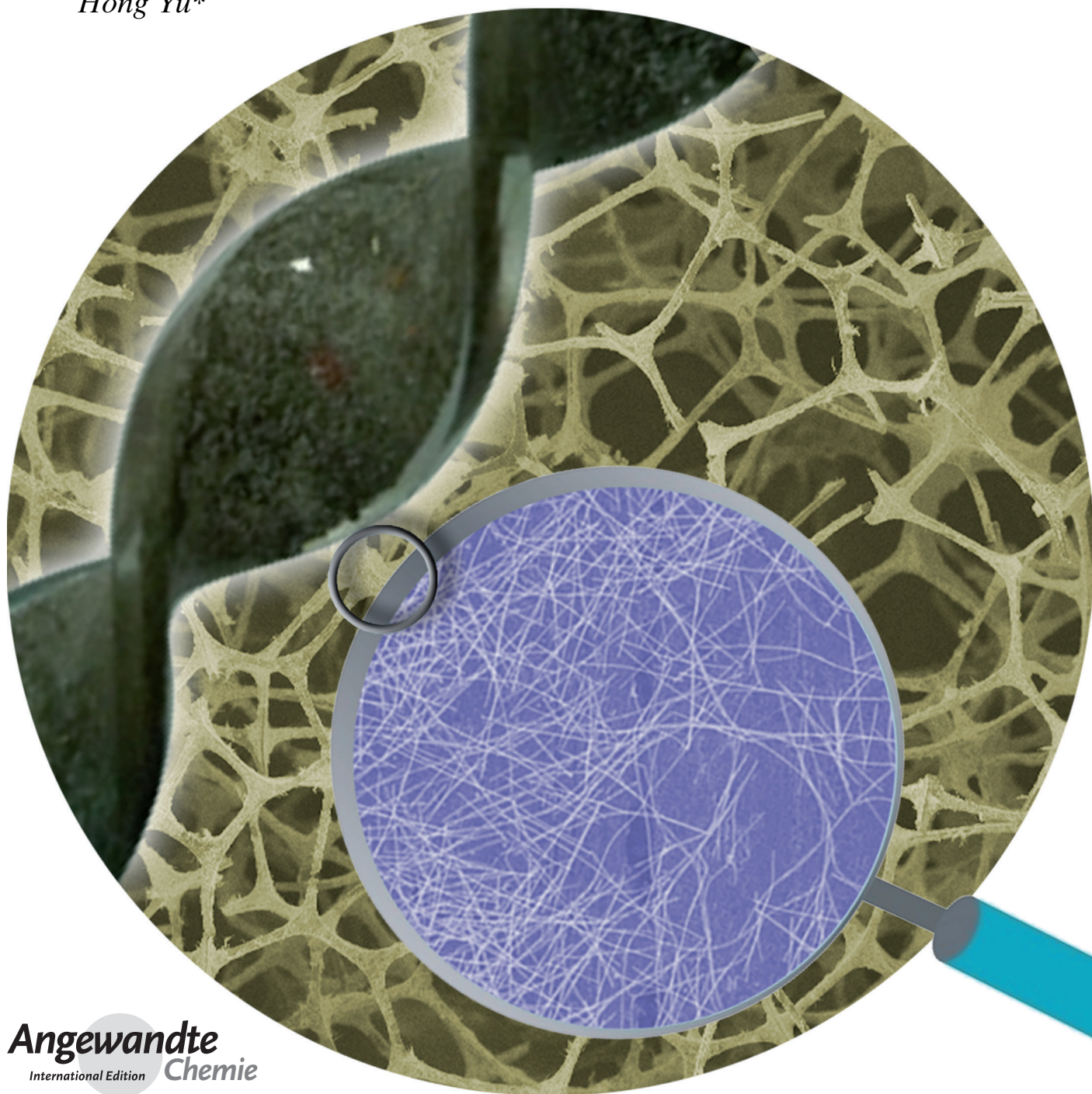


# Stretchable Conductors Based on Silver Nanowires: Improved Performance through a Binary Network Design\*\*

*Jin Ge, Hong-Bin Yao, Xu Wang, Yin-Dong Ye, Jin-Long Wang, Zhen-Yu Wu, Jian-Wei Liu, Feng-Jia Fan, Huai-Ling Gao, Chuan-Lin Zhang, and Shu-Hong Yu\**



Traditional rigid wafer-based electronic conductors can hardly meet the requirement of future flexible electronic devices, including flexible circuitries, artificial skins, flexible sensors and actuators, electronic eye cameras, and stretchable displays,<sup>[1–9]</sup> because they cannot retain high conductivity under substantial stretching and bending deformation. To replace conventional rigid conductors, various types of conductive stretchable materials have recently been designed and fabricated, such as wavy conductive wires or membranes on flexible substrates,<sup>[3,10–13]</sup> conductive nanowire network films,<sup>[14–16]</sup> rigid conductive components embedded or bonded with soft rubbery polymers,<sup>[4,17–19]</sup> and three-dimensional (3D) conductive fillers in poly(dimethylsiloxane)(PDMS).<sup>[20–22]</sup> Recently, to enhance the conductivities of stretchable conductors, conductive interconnected 3D structured materials were prepared and used as conductive components in elastomeric conductors.<sup>[23,24]</sup> The key advantage of such a design is that the interconnected 3D conductive network will maintain elastomericity and conductivity after being incorporated into flexible polymers and the conductivity of these conductors is not substantially reduced by shape deformation before breaking the conductive 3D networks. For example, Cheng et al.<sup>[20]</sup> have fabricated elastomeric conductors with high conductivity and stretchability by infiltrating the interconnected 3D scaffold of graphene foam with PDMS in which the interconnected 3D micro-networks of graphene foams were well retained. More recently, Jeon et al.<sup>[25]</sup> have fabricated 3D nano-network PDMS by proximity-field nanopatterning followed by introducing a liquid-phase eutectic gallium-indium alloy (EGaIn) into the porous channels of the structured PDMS. This elastomeric conductor showed ultrahigh electrical conductivity (ca.  $24\,100\text{ Scm}^{-1}$ ) even at a strain exceeding 200%, with excellent cyclic properties and current-carrying capacities. However, the fabrication procedures of such 3D PDMS are very compli-

cated and the cost of EGaIn alloy is extremely high, which would be a big barrier to produce such stretchable conductors on a large scale. Moreover, the liquid alloy may leak from the polymer shell after long-term use, which would be a potential danger, in that it could short out the whole electronic devices and even cause fires. Lee et al.<sup>[26]</sup> have prepared another stretchable conductive composite film by using an e-beam evaporation process to deposit Ti and Au onto the skeleton of porous PDMS generated by exposing the uncured PDMS layer to a stream of hot pressurized water. Although better stretchability was achieved by the design of porous PDMS, the resistance of the obtained conductors increased rapidly with tensile strain (>300% increase of resistance at 30% strain); the energy-intensive e-beam evaporation process is also a concern.

Highly conductive metallic nanowires, such as silver nanowires (AgNWs)<sup>[27]</sup> and copper nanowires,<sup>[28]</sup> show potential applications in the field of electronic conductors. However, most metallic nanowires research focuses on the flexible transparent conductors as a substitute for indium tin oxide, ignoring their application in stretchable conductors. Lately, Zhu et al.<sup>[29]</sup> have fabricated highly stretchable conductors by embedding Ag nanowire (AgNW) film into a PDMS matrix. The obtained AgNW-PDMS film showed stable resistance in a large strain range of 0–50% owing to the formation of a wave shape in the AgNW-PDMS layer. However, the relatively long AgNWs (10–60  $\mu\text{m}$ ) they used can hardly be synthesized on a big scale for industrial applications owing to the limitations of the smallscale synthetic method. Ko et al.<sup>[14]</sup> have reported highly stretchable conductors with low sheet resistance even under a strain above 460% by using ultralong AgNWs (ca. 500  $\mu\text{m}$ ). Nevertheless, the synthesis of such ultralong AgNWs is complicated and time consuming. Moreover, the two stretchable conductors mentioned above are both based on a 2D network, which does not allow the AgNWs to provide the same high level of conductivity as that in a 3D network under the same strain.


Herein, we report a fabrication method for binary-network-structured polyurethane sponge–Ag nanowire–poly(dimethylsiloxane) (PUS–AgNW–PDMS) stretchable conductors with high performance, which solves all of the problems mentioned above. The key to the construction of the binary network structures lies in the choice of commercial polyurethane (PU) sponge with an interconnected and junction-free macroporous structure as the skeleton to support the 2D AgNW networks. Moreover, the facile dip-coating method we adopted can be easily scaled up, making the practical application of these PUS–AgNW elastomeric conductors in flexible devices possible.

The fabrication method for PUS–AgNW–PDMS stretchable conductors is shown in Figure 1a. First, high-quality AgNWs with length of 4–15  $\mu\text{m}$  were synthesized by a previously reported<sup>[27]</sup> facile and scalable one-pot synthesis (Supporting Information, Figure S1). Next, commercially available PU sponges with 3D-interconnected microfiber networks were used as a skeleton on which to construct the PUS–AgNW conductive sponge. After being dipped into an ethanol solution of the AgNWs, the bare PU sponges were fully infiltrated by the ethanol solution of Ag NWs, owing to

[\*] J. Ge,<sup>[†]</sup> Dr. H. B. Yao,<sup>[†]</sup> X. Wang, Y. D. Ye, J. L. Wang, Z. Y. Wu, Dr. J. W. Liu, F. J. Fan, H. L. Gao, C. L. Zhang, Prof. Dr. S. H. Yu  
Division of Nanomaterials and Chemistry, Hefei National Laboratory for Physical Sciences at Microscale, Department of Chemistry, CAS Key Laboratory of Mechanical Behavior and Design of Materials, the National Synchrotron Radiation Laboratory, University of Science and Technology of China, Hefei Anhui 230026 (P. R. China)  
E-mail: shyu@ustc.edu.cn  
Homepage: <http://staff.ustc.edu.cn/~yulab/>

[†] These authors contributed equally to this work.

[\*\*] This work is supported by the National Basic Research Program of China (2010CB934700), the Ministry of Science and Technology of China (2012BAD32B05-4), the National Natural Science Foundation of China (91022032, 912271032, 21061160492), the Chinese Academy of Sciences (KJZD-EW-M01-1), the International Science & Technology Cooperation Program of China (2010DFA41170), a Principal Investigator Award by the National Synchrotron Radiation Laboratory at the University of Science and Technology of China, and the China Postdoctoral Science Foundation (2012M510160).

 Supporting information for this article, including material synthesis and characterization, SEM images, and resistance stability studies under strain-releasing cycles, is available on the WWW under <http://dx.doi.org/10.1002/anie.201209596>.



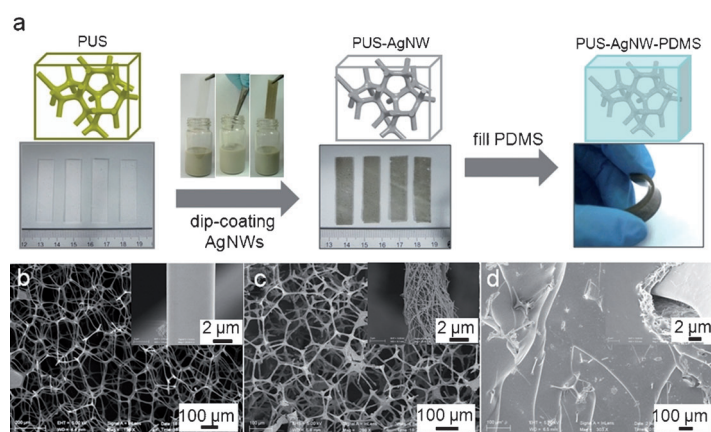


**Figure 1.** a) Fabrication procedure for PUS-AgNW-PDMS stretchable conductors. b–d) SEM images of bare PU sponge, PUS-AgNW, and PUS-AgNW-PDMS composites, respectively.

the hydrophilic surface of the microfibers and the unique macroporous structure of sponges. After evaporating the ethanol, the color of the sponge changed from white to gray (Figure 1a) and the microfibers were uniformly wrapped by the AgNWs (Figure 1c, inset), resulting in a conductive sponge with binary AgNW nano/micro-network structures (Figure 1c). Finally, PDMS was introduced into the PUS-AgNW conductive sponges to form the desired PUS-AgNW-PDMS stretchable conductors. As shown in Figure 1d, the PU microfibers and Ag nanowires are both well encapsulated by PDMS and yield well-defined binary nano/micro-scale network structures, which indicates the significant role of the PUS skeleton in generating the binary-network-structured stretchable conductors. To the best of our knowledge, such a binary network structure (2D nano-network of AgNWs on the PU microfiber surfaces and 3D AgNW micro-networks on the sponge skeleton) has been fabricated for the first time by this facial dip-coating process.

This solution dip-coating method can also feasibly be used for tuning the conductivity of the PUS-AgNW-PDMS conductors by controlling the density of the AgNW coating on the surface of the PU microfiber network through varied dip-coating times and the AgNWs concentration in the ethanol solution. From the SEM images in Figure 2a–d, we can clearly see that the density of AgNWs on the surface of the PU microfibers increases with the number of dip-coatings. Figure 2e illustrates that the mass-content of AgNWs in PU sponges increases almost linearly with the number of dip-coating cycles. At the same time, the

conductivity of the PUS-AgNW also increased linearly from ca.  $8.35 \text{ S cm}^{-1}$  to ca.  $19.20 \text{ S cm}^{-1}$  as the number of dip-coating cycles increases from one to eight (Figure 2f), which demonstrates that various conductive PUS-AgNW composites can be obtained by simply tuning the dip-coating cycle number. Furthermore, the conductivities of PUS-AgNWs remain nearly constant after impregnation of the PUS-AgNW sponge with PDMS (Figure 2f), which means that the binary structures of the AgNWs are maintained during PDMS impregnation and curing. Figure 2g shows that the conductivity of the elastic conductors, which have an ultralow mass content of AgNWs, is very high; our PUS-AgNW-PDMS composites contain only ca. 0.55 wt. % AgNWs, but display a conductivity of up to ca.  $10.25 \text{ S cm}^{-1}$ .

As shown above, we have successfully fabricated elastomeric PUS-AgNW-PDMS conductors containing a binary network, including an interconnected junction-free PU network at the microscale and a AgNW network at the nanoscale. To further explain the function of the binary network structure in our PUS-AgNW-PDMS stretchable conductors with regards to their performance, we undertook an analysis of the structure deformation of PUS-AgNW-PDMS composites during the stretching process. The microstructure variation of PUS-AgNW-PDMS flexible conductors under tensile strength was studied by optical microscope. As shown in Figure 3a–d, as the tensile strain on PUS-AgNW-PDMS increased from 0–100%, the macropores of PU sponge (marked by the yellow window) shrank perpendicular to the direction of the tensile force and elongated in the direction of the applied force. This shape deformation of the PU skeleton at the microscale under a tensile strain of 0–100% guarantees a continuance of the conductive network in the PDMS. It also means that the deformation and elongation of the PU micro-networks would

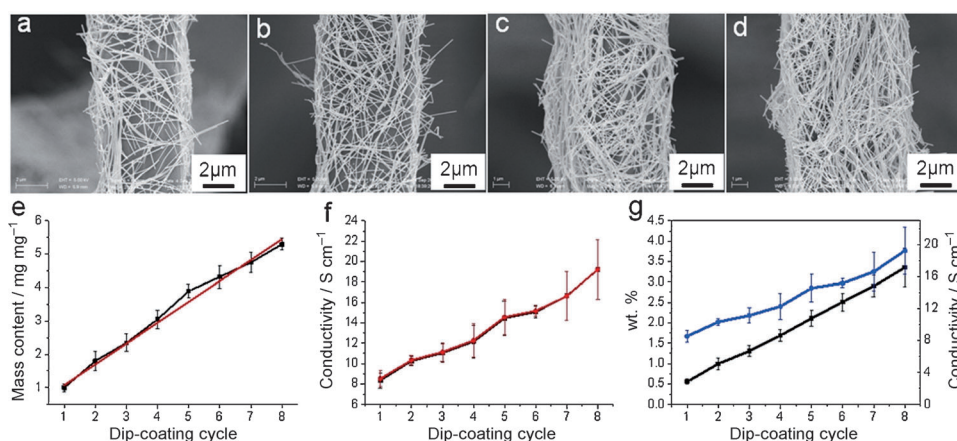


**Figure 2.** a–d) SEM images of the backbone surface of PUS-AgNW composites prepared by dipping a bare PUS into an ethanol solution of AgNWs ( $7.5 \text{ mg mL}^{-1}$ ) one, two, three, and four times, respectively. e) Mass loading of AgNWs on the PUS surface versus number of dip-coating cycles; the red line is drawn as a guide for the eye. f) Electrical conductivity of PUS-AgNW (—■—) and PUS-AgNW-PDMS (—●—) composites as a function of the number of dip-coating cycles. g) Mass content (wt. %; —■—) and electrical conductivity (—●—) of PUS-AgNW-PDMS composites as a function of the number of dip-coating cycles.

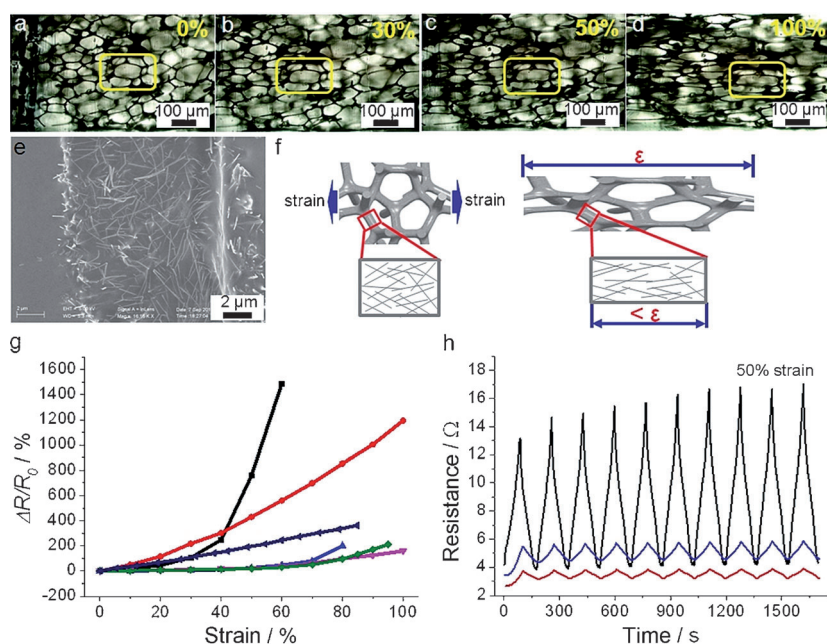


**Figure 3.** a–d) Optical microscope images of PUS-AgNW-PDMS at 0%, 30%, 50%, and 100% strain, respectively. e) SEM image of AgNWs embedded in a PDMS matrix after removal of PU fibers in PUS-AgNW-PDMS composites. f) Illustration of effects of elongation on the PUS-AgNW-PDMS micro-network and the AgNW nano-network (expansions) of the composite under tensile strain ( $\epsilon$ ). g) Variation of normalized resistance ( $\Delta R/R_0$ ) as a function of tensile strain (up to 100% in the first stretch) on PUS-RGO-PDMS (—■—), AgNW-PDMS film (—●—), PUS-AgNW-PDMS (—▼—), and other similar composites reported in the literature: Refs [14] (—▲—), [20] (—◆—), and [29] (—◀—). h) Resistance responses of 2.1 wt.% PUS-AgNW-PDMS (—), 3.3 wt.% PUS-AgNW-PDMS (—), and AgNW-PDMS film (—) to 0–50% strain as a function of time.

protect contacts among AgNWs from quick disconnection, which results in improved performance. At the nanoscale, a fine interconnected AgNW network is formed by AgNWs embedded in PDMS (Figure 3e); such a 2D network can also effectively accommodate the deformation without a significant decay in conductivity under stretching.<sup>[14]</sup>

A binary network model is shown in Figure 3f, which illustrates the deformation mechanism of the binary network during stretching. Although the whole network of stretchable conductors was elongated to a certain strain ( $\epsilon$ ) under the tensile strength of the material, the tensile strain observed in AgNW networks on the surface of the PU micro-skeleton is smaller than  $\epsilon$ , owing to the shape deformation of the PU micro-network. In other words, the tensile strain applied to the AgNW network in PUS-AgNW-PDMS conductive composites was shared by the PU micro-skeleton. Thus AgNW networks in PUS-AgNW-PDMS suffered less stretching than those in AgNW-PDMS films under the same extension. Furthermore, the electrical conductivity of AgNW networks is predominantly determined by the contacts among AgNWs.<sup>[30]</sup> When the AgNW network is stretched, AgNWs would detach from each other, which results in fewer contacts among the AgNWs, thus leading to a decrease in electrical conductivity.<sup>[29]</sup> Therefore, the binary network structure we designed in PUS-AgNW-PDMS composites would improve their performance as stretchable conductors. The stability

enhancement in the electric conductivity of a binary network structure over a single network structure under tensile strain is shown in Figure 3g. The resistance variations of stretchable conductors with different nano/micro-structures were studied as a function of tensile strain from 0–100%. During the first stretching, the resistance increase ( $\Delta R/R_0$ ) of PUS-AgNW-PDMS at the maximum strain (100%) was 160%, which is better than for the AgNW-PDMS film (1190% at 100% strain; Figure S2), PUS-RGO-PDMS composites (1490% at 60% strain; Figure S3), and graphene foam-PDMS<sup>[20]</sup> (ca. 210% at 95% strain), as well as previously reported flexible conductors based on AgNWs: AgNW (10–60  $\mu\text{m}$ ) film embedded in PDMS<sup>[29]</sup> (ca. 360% at 85% strain) and AgNW (ca. 500  $\mu\text{m}$ ) film on non-prestrained Ecoflex substrate<sup>[14]</sup> (ca. 200% at 80% strain). From the viewpoint of micro/nano-structures in these stretchable conductors, we can see that AgNW-PDMS films have no 3D micro-network, only a 2D AgNW network. On the other hand, PUS-RGO-PDMS and graphene-PDMS composites have a 3D graphene micro-network but no 2D nano-network. In this case, it is believed that our conductive binary networks can enhance the performance of stretchable conductors. The resistance fluctuation of PUS-AgNW-PDMS and AgNW-

PDMS stretchable conductors under 50% strain was investigated as well. As shown in Figure 3h, the resistance fluctuation of PUS-AgNW-PDMS is five-fold smaller than that of AgNW-PDMS film. This enhanced electromechanical stability is caused by the binary network structure in our prepared PUS-AgNW-PDMS conductive composite as well. Figure 3g also shows that the PUS-AgNW-PDMS composites with a higher mass loading of AgNWs have better electromechanical stability, which indicates that the resistance stability of the PUS-AgNW-PDMS composites can be further improved by increasing the dipping deposition times of AgNWs on the PU sponge. Moreover, we also observed that the PDMS matrix can make the intrinsically fragile AgNW network more mechanically robust. The influence of PDMS on the resistance stability was investigated through contrast experiments. We coated the PUS-AgNW composites with RGO by dipping these composites into an RGO suspension before impregnation of the PUS-AgNW with PDMS. The RGO was well wrapped onto the AgNWs that coated the surface of the PU microfibers (Figure S4a,b), thus preventing them from transfer into PDMS (Figure S4c). Analysis shows that the electromechanical stability of the PUS-AgNW-RGO-PDMS conductive composites was deteriorated relative to that of PUS-AgNW-PDMS (Figure S4d). The reason for this is that the AgNWs in PUS-AgNW-PDMS, owing to its contact with the PDMS matrix, can return to their

original position and remain in good contact with each other after releasing the tensile strain; however, without the fixation offered by the PDMS matrix, the loose AgNWs on the surface of the PU skeleton will gradually become detached from each other after strain-releasing cycles, resulting in quicker deterioration of conductivity. Furthermore, the PUS-AgNW-PDMS also show a high elongation (140%) before fracture, and the resistance remains very low at the maximum tensile strain (Figure S5).

We also studied the resistance variation of the PUS-AgNW-PDMS flexible conductor under bending deformation. As shown in Figure 4a, during the first bending cycle, the conductivity of PUS-AgNW-PDMS composite had a slight decrease from  $10.1 \text{ S cm}^{-1}$  to  $9.7 \text{ S cm}^{-1}$  at a bending radius of 1.0 mm and then recovered to  $9.78 \text{ S cm}^{-1}$  after unbending. As the bending cycle number increased, the resistance variation of the PUS-AgNW-PDMS composites gradually became stable under bending deformation. As shown in Figure 4b the resistance variation curve at the 1000th cycle is very flat. The conductivity of the PUS-AgNW-PDMS composites under reversible bending cycles was very stable as well, even at up to 10000 bending cycles only a slight decrease in conductivity (9%) was observed. In practice, high performance stretchable conductors not only need to withstand tensile and bending deformation without significant degradation in conductivity, but also need to maintain consistent resistance under varied voltages or currents. Figure 4c shows a typical  $I$ - $V$  response at specific strains of 0%, 30%, and 50%, which clearly exhibits the ohmic properties of devices consisting of LED lights integrated with the stretchable conductors. The pictures (Figure 4c, insets) also show that the brightness of the LED lights exhibited almost no change after

stretching the PUS-AgNW-PDMS conductors to a tensile strain of 50% under constant voltage, which implies that our fabricated conductors could retain constant resistance with different voltages applied while enduring 50% tensile strain. Furthermore, Figure 4d demonstrates that the current-carrying capacity of our conductors could reach up to a high current density of  $1.36 \text{ A cm}^{-2}$ , which makes the composites potentially applicable in flexible high-power electronic devices.

In summary, we have demonstrated a novel binary network structure design to improve the electromechanical performance of stretchable conductors based on AgNWs. The key to constructing a binary network structure is to use commercially available PU sponge with a 3D-conjunction-free micro-network structure as the skeleton for supporting AgNW networks. The polyurethane sponge-Ag nanowire-poly(dimethylsiloxane) (PUS-AgNW-PDMS) stretchable conductors with binary network structures can be prepared through a facile solution-dipping method. The resulting PUS-AgNW-PDMS stretchable conductors exhibit high electrical conductivity (exceeding  $19.2 \text{ S cm}^{-1}$ ) and excellent electromechanical stability under high tensile strain (50%) and a small bend radius (1 mm) owing to the combined effects from the binary network. The scalable fabrication method and low-cost raw materials make these binary network stretchable conductors promising materials for future use in flexible, stretchable, and foldable electronic devices.

Received: November 30, 2012

**Keywords:** binary networks · conducting materials · elastomers · nanostructures · stretchable conductors

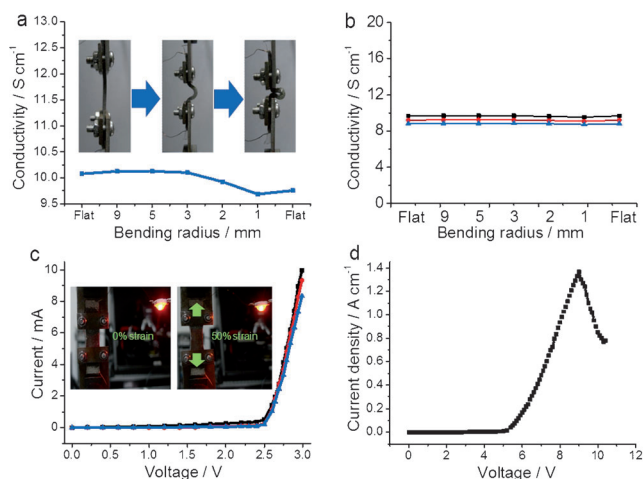


**Figure 4.** a) Conductivity of the composite at a bend radius of up to 1.0 mm in the first bending cycle. The inset pictures describe the bending process. b) Conductivity as a function of bend radius at the 1000th (—■—), 5000th (—●—), and 10000th (—▲—) cycle. c) Current-voltage measurement of elastomeric conductors integrated with an LED at 0% (—■—), 30% (—●—), and 50% (—▲—) strain. The inset photographs show a commercial LED lit using the elastomeric conductors under 0% and 50% strain. d) Current density versus voltage for PUS-AgNW-PDMS integrated with two LEDs.

- [1] Y. Son, J. Yeo, H. Moon, T. W. Lim, S. Hong, K. H. Nam, S. Yoo, C. P. Grigoropoulos, D. Y. Yang, S. H. Ko, *Adv. Mater.* **2011**, 23, 3176.
- [2] K. Takei, T. Takahashi, J. C. Ho, H. Ko, A. G. Gillies, P. W. Leu, R. S. Fearing, A. Javey, *Nat. Mater.* **2010**, 9, 821.
- [3] B. Y. Ahn, E. B. Duoss, M. J. Motala, X. Y. Guo, S. I. Park, Y. J. Xiong, J. Yoon, R. G. Nuzzo, J. A. Rogers, J. A. Lewis, *Science* **2009**, 323, 1590.
- [4] T. Sekitani, Y. Noguchi, K. Hata, T. Fukushima, T. Aida, T. Someya, *Science* **2008**, 321, 1468.
- [5] H. C. Ko, M. P. Stoykovich, J. Z. Song, V. Malyarchuk, W. M. Choi, C. J. Yu, J. B. Geddes, J. L. Xiao, S. D. Wang, Y. G. Huang, J. A. Rogers, *Nature* **2008**, 454, 748.
- [6] T. Sekitani, M. Takamiya, Y. Noguchi, S. Nakano, Y. Kato, T. Sakurai, T. Someya, *Nat. Mater.* **2007**, 6, 413.
- [7] T. Someya, Y. Kato, T. Sekitani, S. Iba, Y. Noguchi, Y. Murase, H. Kawaguchi, T. Sakurai, *Proc. Natl. Acad. Sci. USA* **2005**, 102, 12321.
- [8] T. Someya, T. Sekitani, S. Iba, Y. Kato, H. Kawaguchi, T. Sakurai, *Proc. Natl. Acad. Sci. USA* **2004**, 101, 9966.
- [9] T. Sekitani, H. Nakajima, H. Maeda, T. Fukushima, T. Aida, K. Hata, T. Someya, *Nat. Mater.* **2009**, 8, 494.
- [10] Y. Zhu, F. Xu, *Adv. Mater.* **2012**, 24, 1073.
- [11] X. L. Wang, H. Hu, Y. D. Shen, X. C. Zhou, Z. J. Zheng, *Adv. Mater.* **2011**, 23, 3090.
- [12] D. C. Hyun, M. Park, C. Park, B. Kim, Y. Xia, J. H. Hur, J. M. Kim, J. J. Park, U. Jeong, *Adv. Mater.* **2011**, 23, 2946.
- [13] D. Y. Khang, H. Q. Jiang, Y. Huang, J. A. Rogers, *Science* **2006**, 311, 208.



- [14] P. Lee, J. Lee, H. Lee, J. Yeo, S. Hong, K. H. Nam, D. Lee, S. S. Lee, S. H. Ko, *Adv. Mater.* **2012**, *24*, 3326.
- [15] T. Yamada, Y. Hayamizu, Y. Yamamoto, Y. Yomogida, A. Izadi-Najafabadi, D. N. Futaba, K. Hata, *Nat. Nanotechnol.* **2011**, *6*, 296.
- [16] K. Liu, Y. H. Sun, P. Liu, X. Y. Lin, S. S. Fan, K. L. Jiang, *Adv. Funct. Mater.* **2011**, *21*, 2721.
- [17] Y. Y. Zhang, C. J. Sheehan, J. Y. Zhai, G. F. Zou, H. M. Luo, J. Xiong, Y. T. Zhu, Q. X. Jia, *Adv. Mater.* **2010**, *22*, 3027.
- [18] M. K. Shin, J. Oh, M. Lima, M. E. Kozlov, S. J. Kim, R. H. Baughman, *Adv. Mater.* **2010**, *22*, 2663.
- [19] Z. Yu, X. Niu, Z. Liu, Q. Pei, *Adv. Mater.* **2011**, *23*, 3989.
- [20] Z. P. Chen, W. C. Ren, L. B. Gao, B. L. Liu, S. F. Pei, H. M. Cheng, *Nat. Mater.* **2011**, *10*, 424.
- [21] K. H. Kim, M. Vural, M. F. Islam, *Adv. Mater.* **2011**, *23*, 2865.
- [22] H.-W. Liang, Q.-F. Guan, Z. Zhu, L.-T. Song, H.-B. Yao, X. Lei, S.-H. Yu, *NPG Asia Mater.* **2012**, *4*, e19.
- [23] X. C. Gui, A. Y. Cao, J. Q. Wei, H. B. Li, Y. Jia, Z. Li, L. L. Fan, K. L. Wang, H. W. Zhu, D. H. Wu, *ACS Nano* **2010**, *4*, 2320.
- [24] H. B. Yao, G. Huang, C. H. Cui, X. H. Wang, S. H. Yu, *Adv. Mater.* **2011**, *23*, 3643.
- [25] J. Park, S. D. Wang, M. Li, C. Ahn, J. K. Hyun, D. S. Kim, D. K. Kim, J. A. Rogers, Y. G. Huang, S. Jeon, *Nat. Commun.* **2012**, *3*, 916.
- [26] G. S. Jeong, D.-H. Baek, H. C. Jung, J. H. Song, J. H. Moon, S. W. Hong, I. Y. Kim, S.-H. Lee, *Nat. Commun.* **2012**, *3*, 977.
- [27] C. Yang, H. Gu, W. Lin, M. M. Yuen, C. P. Wong, M. Xiong, B. Gao, *Adv. Mater.* **2011**, *23*, 3052.
- [28] D. Zhang, R. Wang, M. Wen, D. Weng, X. Cui, J. Sun, H. Li, Y. Lu, *J. Am. Chem. Soc.* **2012**, *134*, 14283.
- [29] F. Xu, Y. Zhu, *Adv. Mater.* **2012**, *24*, 5117.
- [30] L. B. Hu, H. S. Kim, J. Y. Lee, P. Peumans, Y. Cui, *ACS Nano* **2010**, *4*, 2955.